Machine Copy for Proofreading, Vol. x, y–z, 2012

AMPLITUDE-ONLY MEASUREMENTS OF A DUAL OPEN ENDED COAXIAL SENSOR SYSTEM FOR DETERMINATION OF COMPLEX PERMITTIVITY OF MATERIALS

Kim Yee Lee[1, *], Boon Kuan Chung[1], Zulkifly Abbas[2], Kok Yeow You[3], and Ee Meng Cheng[4]

[1]Centre for Communication Systems and Networks, Universiti Tunku Abdul Rahman, Kuala Lumpur 53300, Malaysia

[2]Department of Physics, Universiti Putra Malaysia, UPM Serdang 43300, Malaysia

[3]Department of Radio Communication Engineering, Universiti Teknologi Malaysia, UTM, Skudai, Johor 81310, Malaysia

[4]School of Mechatronic Engineering, University Malaysia Perlis, Ulu Pauh Campus, Arau, Perlis 02600, Malaysia

Abstract—This paper describes a novel permittivity measurement technique using dual open ended coaxial sensors. The magnitudes of the reflection coefficient from two open ended coaxial sensors were used to determine complex reflection coefficients and permittivity of a sample under test.

1. INTRODUCTION

Various admittance models of an open ended coaxial sensor have been proposed to determine complex permittivity of materials. These include analytical models such as capacitance, admittance, virtual line and rational function models [1] as well as numerical techniques based on the finite element method, finite difference time domain method and method of moment.

Unfortunately, all the opened ended coaxial models require measured values of complex reflection coefficient to compute permittivity of the material under test. Recently, there has been an increasing demand for a simple equipment to determine complex

Received 29 August 2012.

* Corresponding author: Kim Yee Lee (kylee@utar.edu.my).

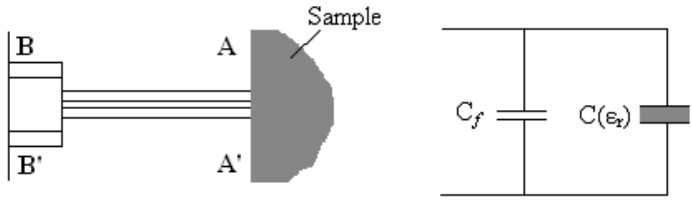

Figure 1. Open ended reflection method, (a) coaxial sensor terminated by a semi-infinite sample, and (b) capacitive equivalent circuit at plane A-A'.

permittivity of materials based on reflection measurements of open ended coaxial sensors [2–7].

This paper presents a dual open ended coaxial sensor system requiring only amplitude measurements of the reflection coefficients from two different open-ended coaxial sensors to calculate the complex permittivity of a sample. An improved capacitance model has been derived to calculate the complex reflection coefficient which in turn is used to determine the complex permittivity of a sample under test.

2. CAPACITANCE MODEL AND MODIFIED CAPACITANCE MODEL

The measurement configuration of the open-ended coaxial sensor and its capacitive equivalent circuit are illustrated in Figures 1(a) and (b), respectively [8]. In this model, the capacitance consists of two parts: $C(\varepsilon_r)$ which is related to the dielectric properties of the sample, and the fringing capacitance C_f which is independent of the dielectric properties of the sample.

The reflection coefficient, Γ of the open ended coaxial sensor at AA' plane is related to the characteristic impedance, Z_0 of the measurement system and the complex relative permittivity, ε_r^* of sample under test in the form

$$\Gamma^* = \Gamma e^{j\Phi} = \frac{1 - j\omega Z_0 \left[C(\varepsilon_r^*) + C_f\right]}{1 + j\omega Z_0 \left[C(\varepsilon_r^*) + C_f\right]} \tag{1}$$

where $C(\varepsilon_r^*) = C_0\varepsilon_r^*$, and C_0 is the capacitance of the capacitor filled with air, C_f is the capacitance independent of the material and ω is the operation angular frequency. The values of C_0 and C_f are found

by calibrating the open ended sensor with a standard sample of known dielectric permittivity, such as, deionized water [9].

Expanding the complex notation in Equation (1) gives:

$$\Gamma^* = \Gamma' + j\Gamma'' = \frac{1 - j\omega Z_0 \left[C_0(\varepsilon_r' + j\varepsilon_r'') + C_f\right]}{1 + j\omega Z_0 \left[C_0(\varepsilon_r' + j\varepsilon_r'') + C_f\right]} \tag{2}$$

where the real and imaginary parts of complex reflection coefficient, Γ^* are expressed as:

$$\Gamma' = \frac{1 + \Gamma''\omega Z_0 C_0 \varepsilon_r' + \omega Z_0 C_0 \varepsilon_r'' + \Gamma''\omega Z_0 C_f}{1 - \omega Z_0 C_0 \varepsilon_r''} \tag{3}$$

$$\Gamma'' = \frac{(1 + \Gamma')(\omega Z_0 C_0 \varepsilon_r' + \omega Z_0 C_f)}{\omega Z_0 C_0 \varepsilon_r'' - 1}. \tag{4}$$

From Equation (2),

$$\varepsilon_r^* = \frac{1 - \Gamma^*}{j\omega Z_0 C_0 \left(1 + \Gamma^*\right)} - \frac{C_f}{C_0} \tag{5}$$

where the real and imaginary parts of ε_r^* are respectively

$$\varepsilon_r' = \frac{-2\Gamma''}{\omega Z_0 C_0 \left(|\Gamma|^2 + 2\Gamma' + 1\right)} - \frac{C_f}{C_0} \tag{6}$$

$$\varepsilon_r'' = \frac{|\Gamma|^2 - 1}{\omega Z_0 C_0 \left(|\Gamma|^2 + 2\Gamma' + 1\right)} \tag{7}$$

By substituting of Equations (6) and (7) into Equations (3) and (4), they can be represented as:

$$\Gamma' = \frac{|\Gamma|^2 - 1 - \omega Z_0 C_0 \varepsilon_r'' \left(1 + |\Gamma|^2\right)}{2\omega Z_0 C_0 \varepsilon_r''} \quad \text{(Real)} \tag{8}$$

$$\Gamma'' = \frac{(C_0 \varepsilon_r' + C_f)\left(1 - |\Gamma|^2\right)}{2C_0 \varepsilon_r''} \quad \text{(Imaginary)} \tag{9}$$

Equations (8) and (9) suggest the real and imaginary part of Γ are amplitude dependent and independent of the phase of the reflection coefficient.

The fringing field capacitance C_f is independent of the permittivity of material under tests ε_r^*. Assuming $C_f = 0$ and substituting Equations (8) and (9) into Equation (4) leads to

$$\frac{C_0 \varepsilon'_{app}\left(1 - |\Gamma|^2\right)}{2C_0 \varepsilon''_{app}} = \frac{\left(1 + \frac{|\Gamma|^2 - 1 - \omega Z_0 C_0 \varepsilon''_{app}\left(1 + |\Gamma|^2\right)}{2\omega Z_0 C_0 \varepsilon''_{app}}\right) \omega Z_0 C_0 \varepsilon'_{app}}{\omega Z_0 C_0 \varepsilon''_{app} - 1} \tag{10}$$

ε'_r and ε''_r in Equation (4) are replaced with an apparent dielectric constant ε'_{app} and loss factor ε''_{app}, respectively in Equation (10).

Rearranging Equation (10) in the form

$$\begin{aligned}&\left(2\omega Z_0 C_0 + 2\omega Z_0 C_0 |\Gamma|^2\right)\varepsilon''_{app} + \left(\omega Z_0 C_0 - \omega Z_0 C_0 |\Gamma|^2\right)\left(\varepsilon'^2_{app} + \varepsilon''^2_{app}\right)\\ &= \left(|\Gamma|^2 - 1\right)\end{aligned} \tag{11}$$

Allows matrix representation of two sets of measurement data

$$\begin{aligned}&\begin{bmatrix} 2\omega Z_0 C_{01} + 2\omega Z_0 C_{01} |\Gamma_1|^2 & \omega Z_0 C_{01} - \omega Z_0 C_{01} |\Gamma_1|^2 \\ 2\omega Z_0 C_{02} + 2\omega Z_0 C_{02} |\Gamma_2|^2 & \omega Z_0 C_{02} - \omega Z_0 C_{02} |\Gamma_2|^2 \end{bmatrix} \begin{bmatrix} \varepsilon''_{app} \\ \varepsilon'^2_{app} + \varepsilon''^2_{app} \end{bmatrix}\\ &= \begin{bmatrix} |\Gamma_1|^2 - 1 \\ |\Gamma_2|^2 - 1 \end{bmatrix}\end{aligned} \tag{12}$$

Leading to

$$\varepsilon''_{app} = \frac{\left(C_{02}^2 - C_{01}^2\right)\left(|\Gamma_1|^2 - 1\right)\left(1 - |\Gamma_2|^2\right)}{2\omega Z_0 C_{02} C_{01}\left(C_{02}\left(1 + |\Gamma_1|^2\right)\left(1 - |\Gamma_2|^2\right) - C_{01}\left(1 + |\Gamma_2|^2\right)\left(1 - |\Gamma_1|^2\right)\right)} \tag{13}$$

And

$$\varepsilon'^2_{app} + \varepsilon''^2_{app} = \frac{C_{02}\left(|\Gamma_1|^2 - 1\right)\left(1 + |\Gamma_2|^2\right) - C_{01}\left(|\Gamma_2|^2 - 1\right)\left(1 + |\Gamma_1|^2\right)}{\omega^2 Z_0^2 C_{02} C_{01}\left(C_{01}\left(1 - |\Gamma_1|^2\right)\left(1 + |\Gamma_2|^2\right) - C_{02}\left(1 - |\Gamma_2|^2\right)\left(1 + |\Gamma_1|^2\right)\right)} \tag{14}$$

where

$$\varepsilon'_{app} = \sqrt{\left(\varepsilon'_{app}\right)^2 + \left(\varepsilon''_{app}\right)^2 - \varepsilon''^2_{app}} \tag{15}$$

The real and imaginary parts of the complex reflection coefficient Γ can now be calculated by replacing ε'' with ε''_{app} and ε'' with ε''_{app} in Equation (8) and Equation (9) respectively,

$$\Gamma' = \frac{|\Gamma|^2 - 1 - \omega Z_0 C_0 \varepsilon''_{app}\left(1 + |\Gamma|^2\right)}{2\omega Z_0 C_0 \varepsilon''_{app}} \quad \text{(Real)} \tag{16}$$

$$\Gamma'' = \frac{C_0 \varepsilon'_{app}\left(1 - |\Gamma|^2\right)}{2C_0 \varepsilon''_{app}} \quad \text{(Imaginary)} \tag{17}$$

Hence both the real Γ' and imaginary Γ'' parts of the reflection coefficient in Equations (16) and (17) can be calculated in conjunction with Equations (13) and (15) by measuring only the magnitudes $|\Gamma|^2$ of two different open ended coaxial sensors system.

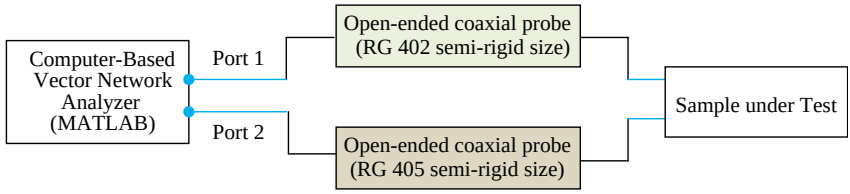

(a)

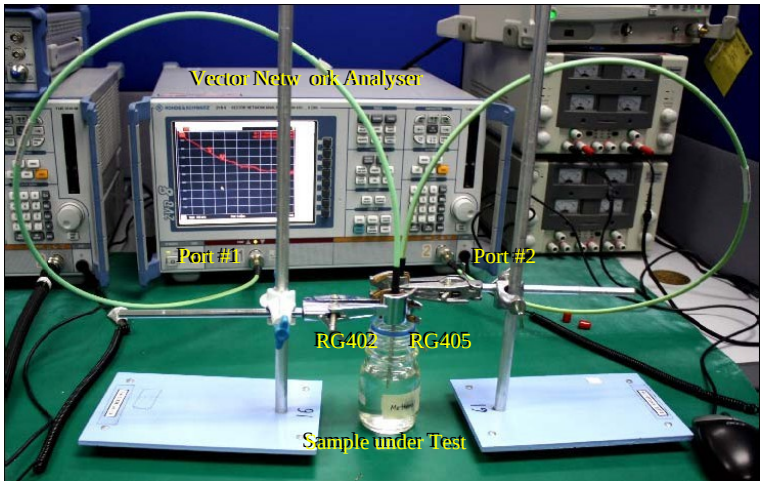

(b)

(c)

Figure 2. (a) Measurement block diagram. (b) Measurement setup. (c) RG402 and RG405 open ended coaxial sensors.

3. MEASUREMENT SYSTEM

The measurement setup shown in Figure 2 consists of a Rohde-Schwarz ZVA8 Vector Network analyzer (VNA) and two open ended coaxial sensors fabricated from commercial RG402 and RG405 semi-rigid

cables. The RG402 semi-rigid cable has an inner and outer conductor radius $a = 0.4572\,\text{mm}$ and $b = 1.5113\,\text{mm}$, respectively. In contrast, the RG405 semi-rigid cable has smaller inner and outer conductor radius $a = 0.2552\,\text{mm}$ and $b = 0.8382\,\text{mm}$. The VNA was in default configuration setting with 201 points, 0 dBm, and CW mode. The VNA was connected to both sensors via two LL142 50 ohm 18 GHz low loss coaxial cables. The amplitude of the reflection coefficient, $|\Gamma_1|^2$ and $|\Gamma_2|^2$ for both the RG402 and RG405 coaxial sensor, respectively were measured in the frequency range between 300 kHz and 8 GHz. All measurements were conducted in ambient temperature of 25°C. The minimum separation distance between the two sensors were kept more than half wavelengths of the operating frequency to avoid coupling. Since it was difficult to calibrate at plane A-A' of the sensor, the port extension technique was applied to extend the calibration plane to the reference plane. Both $|\Gamma_1|^2$ and $|\Gamma_2|^2$ were normalized values with respect to the unloaded sensor (i.e., without sample).

All data storage and computation were implemented in the computer-based VNA. The reflection coefficient magnitude and phase of the sample can be calculated from the measured magnitude $|\Gamma_1|^2$ and $|\Gamma_2|^2$ using Equations (16) and (17) in conjunction with Equations (13) and (15).

For calculation of complex permittivity, the capacitance model was used. Modified capacitance is used particularly for calculation of apparent permittivity which ignoring the fringing field capacitance C_f. It cannot be use because will cause some error since C_f is assumed to be zero. The calculated reflection coefficient in Equations (16) and (17) were then used to determine the permittivity of the sample under test using Equations (6) and (7). The values of $C_0 = 1.953\varepsilon_0(b-a)$ and $C_f = 0.0404\varepsilon_0(b-a)$ were used, where b and a are outer and inner radii of the open ended coaxial sensor.

For comparison purposes, a set of complex reflection coefficient was measured using VNA. The VNA was calibrated using standard two-port TRL calibration.

4. RESULTS AND DISCUSSIONS

The experimental and theoretical calculated reflection coefficient for both RG402 and RG405 type sensors were compared to VNA measurements. Figures 3, 4 and 5 show the comparison for water, methanol and ethanol respectively. Theoretical means calculated reflection coefficient of the sensor using Equations (16) and (17) by permittivity values obtained from Debye model [10, 11]. While experimental (this work) means calculated reflection coefficient

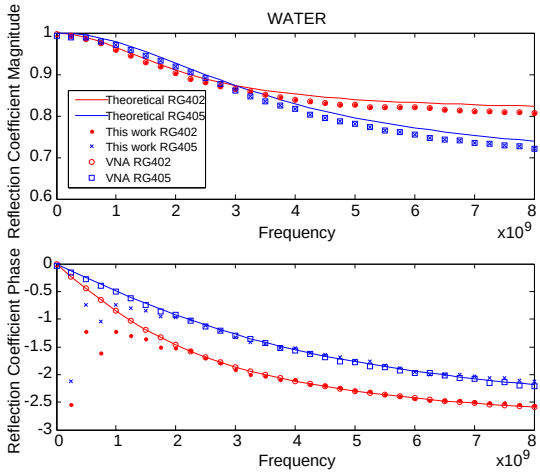

Figure 3. Reflection coefficient of water.

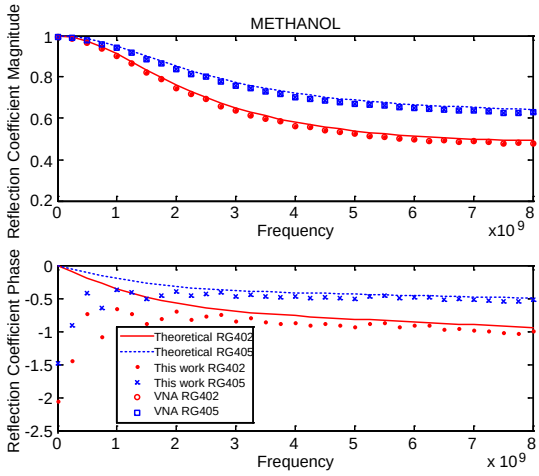

Figure 4. Reflection coefficient of methanol.

obtained by Equations (16) and (17) using magnitude reflection coefficient measured by VNA. And VNA means the complex reflection coefficient measured by calibrated VNA. Magnitudes of the experimental were exactly similar to the VNA since both were measured by VNA. Theoretical calculated reflection coefficient magnitudes have slightly difference due to permittivity values obtained from Debye model.

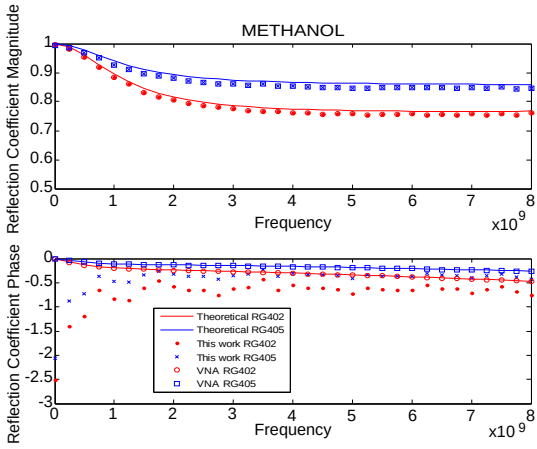

Figure 5. Reflection coefficient of ethanol.

In Figure 3, phase was in good agreement for theoretical calculated RG402 and RG405 sensors when compared to VNA measurements. Errors occurred in frequency less than 2 GHz for experimental results. The high deviation between the experimental and theoretical calculated reflection coefficient values at low frequencies were due to the used of the derivation of Equations (16) and (17). The changes in lower frequency are smaller and lead to difficulties in detecting reflection coefficient magnitude differences between two used sensors in practical.

Figure 4 illustrated reflection coefficients phase for methanol was in good agreement for theoretical and VNA measurement. Same error occurred for frequency less than 3 GHz in experimental results. The error of reflection coefficient phase decreases with the increasing of frequency for both RG402 and RG405 sensors.

Figure 5 illustrated reflection coefficients for ethanol. Good agreement between theoretical and VNA measurement. The error of reflection coefficient phase decreases with the increasing frequency. Similar to methanol in Figure 4, the reason of bigger error in ethanol measurement is because it has lower permittivity value compared to the methanol liquid. It can be clearly seen that, the accuracy for reflection coefficient phase increases with the increasing operation frequency and the permittivity value.

The calculated complex reflection coefficient was used to determine the relative permittivity of sample by using Equations (6) and (7). It was in good agreement with Debye model for water measurement above 2 GHz as illustrated in Figure 6. The error

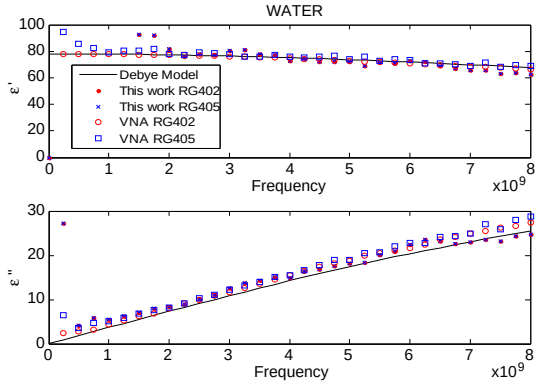

Figure 6. Theoretical and measurements permittivity of water.

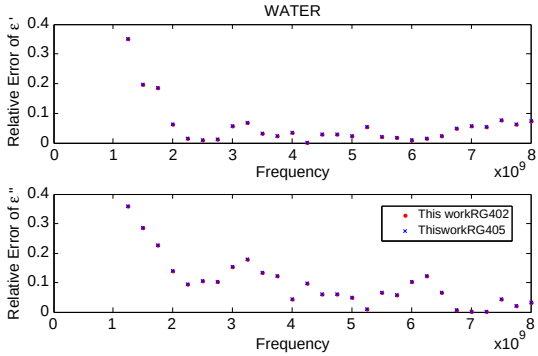

Figure 7. Error of water permittivity measurements.

at frequencies below 2 GHz is contributed by the error in reflection coefficient phase calculation as discuss previously.

The measured relative error of water permittivity for frequency after 2 GHz are less than 0.1 and 0.2 for ε' (dielectric constant) and ε'' (loss tangent) respectively as shown in Figure 7.

The measured complex permittivity of the methanol was in good agreement with Debye model and VNA measurements as illustrated in Figure 8. Both RG402 and RG405 coaxial sensors able perform accurate permittivity measurement for frequency more than 3 GHz.

The relative errors for frequency above 3 GHz are less than 0.25 and 0.1 for ε' and ε'' respectively, as shown in Figure 9. The error decreases with the increasing frequency.

The measured ε' of the ethanol was slightly higher if compared to VNA measurement and Debye model for both RG402 and RG405

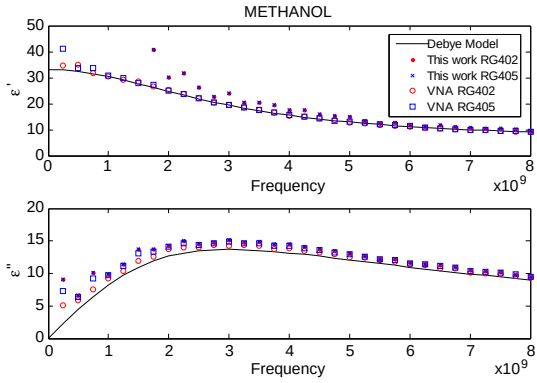

Figure 8. Theoretical and measurements permittivity of methanol.

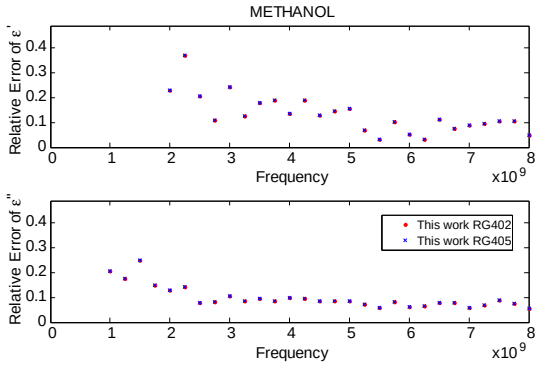

Figure 9. Error of methanol permittivity measurements.

coaxial sensors as illustrated in Figure 10. The error is decreases with the increasing frequency. On the other hand, the measured ε' of the ethanol was in good agreement with theoretical and VNA measurements. Both RG402 and RG405 able perform accurate ε'' measurement for frequency more than 3 GHz.

The relative errors for ethanol measurements are typically 1.50 and 0.15 for ε' and ε'' respectively above 3 GHz as shown in Figure 11. The error slowly decreases with the increasing frequency.

Overall, the relative error for the ε'' was remained low even the values of sample's permittivity is small. In contrast, the relative error in ε' increases significantly when the permittivity of sample is decreased. It shows the constraint of this method which is less accurate especially when the permittivity value of sample under test is low. The

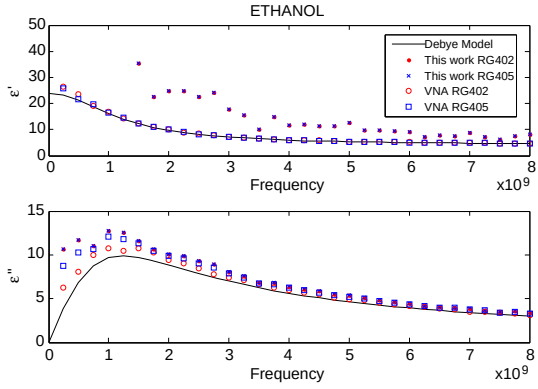

Figure 10. Theoretical and measurements permittivity of ethanol.

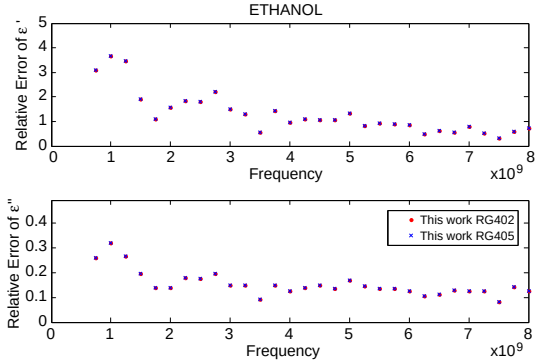

Figure 11. Error of ethanol permittivity measurements.

ε' produces higher error compared to the ε'' is due to higher accumulate errors from both Γ' and Γ'' for dielectric constant calculation as in Equation (6). On the other hand, only Γ'' contribute to error for ε'' calculation as in Equation (7).

5. CONCLUSION

It was found that the suggested dual open-ended coaxial technique provides alternative method to determine complex reflection coefficient by using two magnitude measurements. It also showed that one able to determine permittivity of a sample using two magnitudes from two different sizes of open ended coaxial sensors. The proposed solution is very attractive because of the low cost and simple measuring devices.

This method, due to large measurement error, is only useful for the measurements of liquids with high permittivity value or with water content above 50%.

ACKNOWLEDGMENT

Authors wish to acknowledge the Universiti Tunku Abdul Rahman for the financial support through the UTAR Research Fund (UTARRF/C2-10/L3).

REFERENCES

1. Berube, D. and F. M. Ghannouchi, "A comparative study of four open-ended coaxial sensor models for permittivity measurements of lossy dielectric/biological materials at microwave frequency," *IEEE Trans. Microwave Theory and Techniques*, Vol. 44, No. 10, 1928–1934, 1996.
2. Wang, Y. and M. N. Afsar, "Measurement of complex permittivity of liquids using waveguide techniques," *Progress In Electromagnetics Research*, Vol. 42, 131–142, 2003.
3. Sokoll, T. and A. F. Jacob, "In-situ moisture detection system with a vector network analyser," *Meas. Sci. Tech.*, Vol. 18, No. 4, 1088–1093, 2007.
4. Hasar, U. C., "Permittivity determination of fresh cement-based materials by an open-ended waveguide probe using amplitude-only measurements," *Progress In Electromagnetics Research*, Vol. 97, 27–43, 2009.
5. Hasar, U. C. and O. Simsek, "An accurate complex permittivity method for thin dielectric materials," *Progress In Electromagnetics Research*, Vol. 91, 123–138, 2009.
6. Lee, K. Y., Z. Abbas, Y. K. Yeow, M. D. Nur Sharizan, and C. E. Meng, "In situ measurements of complex permittivity and moisture content in oil palm fruit," *The European Physical Journal — Applied Physics,* Vol. 49, No. 3, 2010.
7. Chen, Q., K.-M. Huang, X. Yang, M. Luo, and H. Zhu, "An artificial nerve network realization in the measurement of material permittivity," *Progress In Electromagnetics Research*, Vol. 116, 347–361, 2011.
8. Gajda, G. and S. S. Stuchly, "An equivalent circuit of an open-ended coaxial line," *IEEE Trans. Instrum. Meas.*, Vol. 32, No. 4, 506–508, 1983.

9. Ghannouchi, F. M., R. G. Bosisio, Y. Demers, and R. Guay, "Computer aided measurement of dielectric properties of saline solutions using a six-port reflecometer," *IEEE Trans. Instrum. Meas.*, Vol. 38, No. 2, 505–508, 1989.
10. Kaatze, U., "Reference liquids for the calibration of dielectric sensors and measurement instrumentals," *Meas. Sci. Tech.*, Vol. 18, No. 4, 967–976, 2007.
11. Misra, D., M. Chabbra, B. R. Epstein, M. Mirotznik, and K. R. Foster, "Noninvasive electrical characterization of materials at microwave frequencies using an open-ended coaxial line: Test of an improved calibration technique," *IEEE Trans. Microwave Theory and Techniques*, Vol. 38, No. 1, 8–14, Jan. 1990.